Results in Control and Optimization 16 (2024) 100449

Contents lists available at ScienceDirect

Results in Control and Optimization

journal homepage: www.elsevier.com/locate/rico

A new analytical study of prey–predator dynamical systems involving the effects of Hide-and-Escape and predation skill augmentation

Warif B. Bassim [a,b], Abdulghafoor J. Salem [a], Ali Hasan Ali [c,*]

[a] Department of Mathematics, College of Computer Science and Mathematics, University of Mosul, Mosul 41001, Iraq
[b] Nineveh Education Directorate, Ministry of Education, Nineveh, Iraq
[c] Institute of Mathematics, University of Debrecen, Pf. 400, H-4002 Debrecen, Hungary

ARTICLE INFO

MSC:
34A34
34D05
92B99
92-10

Keywords:
Prey–predator system
Stability
Local bifurcation
Kolmogorov analysis
Functional response

ABSTRACT

The aim of this work is to provide a comprehensive analysis of the dynamics within an ecosystem characterized by interactions between prey and predators, through a combination of theoretical analysis and numerical simulation. The study investigates the impact of two pivotal effects: the "Hide-and-Escape" behavior exhibited by prey and the "Predation Skill Augmentation" strategy adopted by predators. Theoretical analysis identifies three equilibrium points, all of which show positive characteristics. Furthermore, local stability conditions are determined for each of these equilibrium points. The derivation of global stability conditions is also presented, and their validity and importance as local stability conditions for the coexistence point are demonstrated. In addition, Kolmogorov conditions for coexistence and extinction are verified, as well as local bifurcation analysis. For the validity of the results, a numerical simulation of the system using MATLAB is conducted.

1. Introduction

The study of interactions among competing entities holds significant importance. These interactions have the potential to be utilized in various disciplines within the applied sciences, including but not limited to chemistry, physics, engineering, and ecology [1]. This area of study has attracted considerable attention from a multitude of researchers, particularly from a mathematical standpoint. Lotka [2] and Volterra [3] laid the groundwork for studying these types of interactions by utilizing nonlinear differential equations to mathematically represent the dynamics between prey and predator in ecological systems. This model served as a source of inspiration for numerous researchers in this field, motivating them to conduct extensive research and studies with the objective of enhancing the accuracy of the model by incorporating various effects that simulate real-life organism dynamics.

Functional and numerical responses are fundamental components in the study and modeling of prey–predator dynamics. These components offer valuable insights into the intricacies and interconnections within ecosystems, yielding significant implications for the fields of conservation and ecosystem management [4]. The term "functional response" refers to the manner in which a predator's consumption rate of prey changes in response to variations in prey abundance. Essentially, it measures the efficiency of a predator across different densities of prey [5]. Researchers have identified three primary types of functional responses. Holling Type I functional response is characterized by a linear relationship, implying a consistent rate of prey consumption regardless of prey density. Conversely, Holling Type II functional response displays a saturating curve, indicating a decrease in consumption rate per

* Corresponding author.
E-mail addresses: warifb@gmail.com (W.B. Bassim), drabdul_salim@uomosul.edu.iq (A.J. Salem), ali.hasan@science.unideb.hu (A.H. Ali).

https://doi.org/10.1016/j.rico.2024.100449
Received 20 March 2024; Received in revised form 3 June 2024; Accepted 20 June 2024
Available online 25 June 2024

predator as prey density increases. Holling Type III functional response shows a sigmoidal pattern, suggesting that the consumption rate first rises at low prey densities and then slows as prey density continues to increase [6].

On the other hand, the numerical response related to the aforementioned functional response clarifies how the predator population changes in response to fluctuations in prey density. Essentially, the numerical response examines the correlation between predator reproductive rates and population density concerning the availability of prey [7]. An increase in prey density can lead to a subsequent rise in the predator population over time, due to enhanced carrying capacity. Conversely, a decrease in prey density might result in a decline in the predator population because of reduced food availability.

By incorporating both functional and numerical responses, researchers have been able to develop comprehensive models that offer a more accurate representation of the intricate dynamics involved in prey–predator interactions. The understanding of species population dynamics, prediction of ecosystem change consequences, and development of efficient conservation strategies all hinge on this aspect [8].

Over the past years, several responses have been proposed by researchers such as Lvlev [9], DeAngelis [10], HassellVarley [11], and others. Current literature places emphasis on external factors that exert influence but are absent in functional and numerical responses. In 2017, Li and Wu conducted a study to investigate the stability of the prey–predator model in the presence of prey-protected areas and its influence on the prey's growth rate [12]. In 2019, Pal et al. delved into the dynamics of the prey–predator model, particularly focusing on scenarios that include cooperative hunting strategies among predators [13]. Sekerci, in 2020, examined the effects of climate change on the stability of the prey–predator model [14], while Emery and Mills studied variations in population growth within the same model, emphasizing the impact of predation pressure from predators on prey [15]. Al Basir et al. in 2021, focused on the stability and bifurcation observed in a prey–predator model affected by disease, using the Holling Type II functional response as their theoretical framework [16]. Also in 2021, Jayaprakasha and Baishya researched the effects of toxicity on a prey–predator model, applying the Holling Type I functional response in their study [17], and Lemnaouar et al. concentrated on the stability of the prey–predator model in the context of harvesting, employing the Holling Type IV functional response [18]. Saja and Shireen, in 2022, analyzed the effects of polluted environments on the dynamics of a prey–predator model using the Holling Type I functional response [19]. Lastly, Ghassan et al. in 2023, explored the influence of the rescue effect on prey populations in the prey–predator model, referencing the Holling Type II functional response [20]. Further studies about the stability and the bifurcation analysis can be seen in [21–26].

According to the literature review, developing a prey–predator model by adding a new effect is considered a major challenge for researchers for two reasons. First, selecting a specific effect that has tangible biological meaning in real environments and then modeling it mathematically to provide a realistic representation of this effect poses significant difficulties. Second, integrating this factor into the prey–predator model in a correct and competitive manner, and using mathematical analysis tools to examine the dynamics after adding the factor, are crucial for improving the ability to manage and preserve ecosystems. Based on what the previously mentioned, the objective of this paper is to develop the deterministic prey–predator model, that was presented by Lotka and Volterra by adding two new effects on the model: "Predation Skill Augmentation Effect" for predator and "Hide-and-Escape Effect" for prey. Therefore, the contributions can be summarized in the following points:

- Improving the prey and predator model by proposing two new effects with an explanation of their biological influence and how this explanation was converted into a mathematical equation and integrated into Holling Type II prey predator model in a competitive manner.
- Presenting a comprehensive study of the deterministic model by finding the boundedness of the model and studying the local and global stability of its equilibrium points. Also, explain some cases of local bifurcation. As well as clarifying the conditions of Kolmogorov for coexistence and extinction.
- Simulating the model numerically through MATLAB to compare it with the original one before the addition, as well as explaining how the numerical and theoretical results are harmonious, which indicates the validity of the model and the accuracy of the analysis.

The rest of the paper is organized as follows: Section 2 introduces the proposed model, Section 3 covers the boundedness of the model. The equilibrium points and their stability are discussed in Section 4. Section 5 addresses the Kolmogorov conditions for coexistence, while Section 6 presents the local bifurcation. Numerical simulations and extensive discussions of results are presented in Section 7. Finally, Section 8 provides the conclusion of the paper.

2. New effects and the proposed model

The complex interplay between predators and prey has long been a central focus of research in the field of ecology. This dynamic relationship is shaped by two pivotal factors: the "Predation Skill Augmentation Effect" and the "Hide-andEscape Effect". The former pertains to the enhancement of a predator's hunting skills through accumulated experience [27], and the latter denotes the oscillated capability of prey to avoid being captured by the predator [28].

The effect known as the "Predation Skill Augmentation Effect" refers to the dynamism that a predator acquires through its long-term interaction with prey, leading to an increase in its hunting capabilities. According to Biro et al. [29], extended encounters with prey species not only enhance the predator's ability to capture them but also enable the development of specialized hunting strategies that effectively counteract the prey's defence mechanisms. Therefore, the improvement in predator abilities has a significant influence on the dynamics between predators and prey, and has the potential to determine the stability of the ecosystem [27].

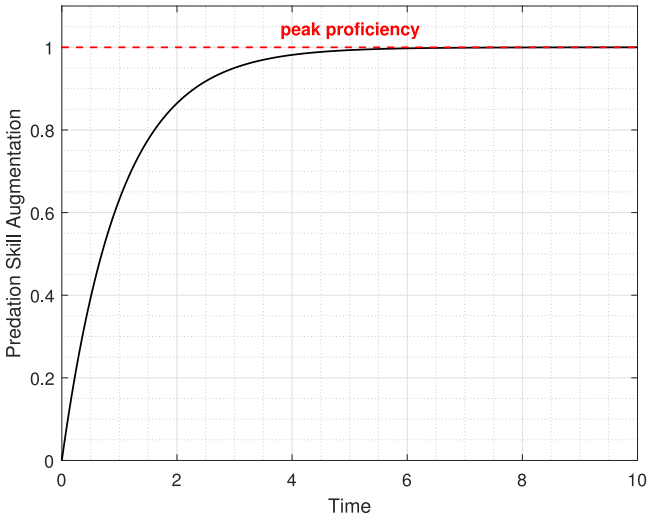

Fig. 1. The evolution of predation skill over time.

On the other hand, the "Hide-and-Escape Effect" encompasses the capability of prey to evade its predators, where this capability is appeared fluctuation. The fluctuations arise due to the limited availability of escape and concealment mechanisms for the prey, where it can get increased or decreased due to the influence of various factors, including variability in environmental conditions, seasonal changes, the health status of the prey, and fluctuations in predator behavior [30]. Mathematically, this oscillating ability can be represented using Brownian motion. However, since the proposed model is deterministic, the cosine function was chosen to lend a more realistic portrayal of this inconsistent survival mechanism within predator–prey models. Further details will be elucidated later in this section.

The simultaneous occurrence of these two effects sheds light on the complex interaction between predators and prey, as both entities constantly adapting their strategies in reaction to each other. The inclusion of these effects in ecological models enhances the precision of comprehending prey–predator dynamics and makes substantial contributions to predictions regarding the stability of ecosystems and the management of species conservation endeavors.

Since the predation skill augmentation is usually non-existent initially and increases over time, the following function has been chosen to model it:

$$j\,(1 - e^{-y}),$$

where $y = y(t)$ is the density of predator, j is a positive parameter that represents the proportion of predators that are able to gain predation skill, and t is the time. It is clear that $j\,(1 - e^{-y}) \in [0, j]$ if y is non-negative.

The choice of the exponential function was predicated upon its intrinsic ability to encapsulate the progression of skill acquisition. As mentioned earlier, the improvement of the predator in hunting acumen tends to evolve incrementally with accumulated experience, and this enhancement is not typically linear. During the early stages of the life of the predator or when introduced to a new environment or prey, there can often be a phase of rapid skill acquisition. However, as the predator gains expertise, the rate of skill development may slow down, embodying the principle of diminishing returns. This complex trajectory is astutely captured by the exponential function, which characterizes a swift increase in growth rate initially that progressively decelerates as the predator nears its peak proficiency. Therefore, the exponential function works as an echo of the empirically observed learning curve in predators within ecological systems as illustrated in Fig. 1.

On the other hand, since the Hide-and-Escape effect oscillates, the cosine function was chosen to represent it as follows:

$$m(1 + \varpi \cos(\sigma x)),$$

where $x = x(t)$ represents the prey density, m is a positive parameter denote to the proportion of preys that had an opportunity to escape away or hide, ϖ is the fluctuation degree, σ is the angular frequency of the fluctuations, and t is the time.

The cosine function was selected to represent the "Hide-and-Escape Effect" due to its periodic nature, making it appropriate for illustrating oscillating behaviors commonly observed in ecological systems. Mathematically, the cosine function oscillates between -1 and 1, making it ideal for portraying periodic variations, such as the fluctuating ability of prey to hide or escape. Specifically, the peak of the function signifies moments when the evasive of the prey capacities are heightened, while its troughs indicate periods of diminished escape capabilities. Furthermore, if parameters ϖ and σ are time-dependent, this can modulate the amplitude of fluctuations over time, offering a deterministic approximation to random behaviors of Brownian motion. The cyclical pattern of the cosine function closely reflects the natural fluctuations in the evasive strategies of the prey, which might be shaped by many elements such as diurnal cycles, seasonal transitions, or shifting environmental stresses. Thus, the cosine function stands as an

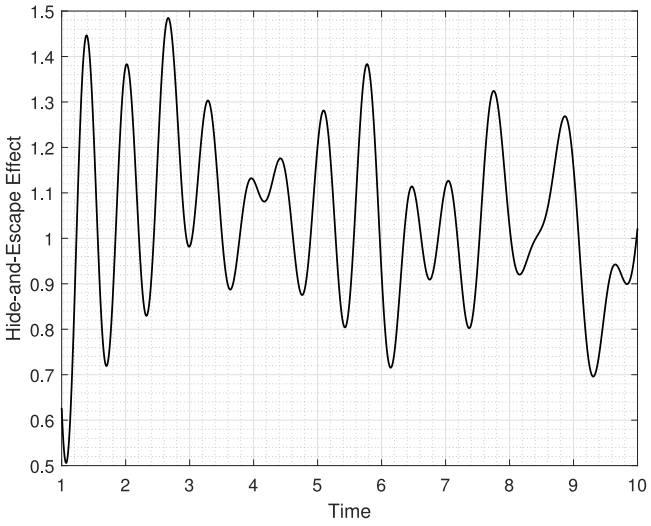

Fig. 2. The behavior of Hide-and-Escape function where ϖ and σ are time-dependent.

Table 1
The components and their meanings in model (2).

The component	Ecological meaning
x	Prey density
y	Predator density
r	The growth rate of prey
a	Predation rate
u	Predator decay rate
h	Half-saturation constant
e	Conversion efficiency
k	Carrying capacity of prey
j	The proportion of predators that are able to gain predation skill
m	The proportion of preys that had an opportunity to escape away or hide

effective mathematical representation to capture the temporal dynamics and unpredictability in the defensive tactics of the prey as illustrated in Fig. 2.

By combining these two effects in interaction manner to an autonomous logistical prey–predator model with functional response $F(x)$ and numerical response $N(x)$, the following model (1) will be obtained:

$$\begin{aligned} \frac{dx}{dt} &= rx\left(1-\frac{x}{k}\right) - F(x)y - j\left(1-e^{-y}\right)x \\ \frac{dy}{dt} &= N(x)y\left(1-\frac{y}{k_y}\right) - uy - m(1+\varpi\cos(\sigma x)), \end{aligned} \tag{1}$$

where the functional and numerical responses used are Holling Type II, defined as $F(x) = \frac{ax}{1+ahx}$ and $N(x) = \frac{eax}{1+ahx'}$, (see [20]).

Additionally, it was assumed that $\varpi = \sigma = 1$, and the carrying capacity of the predator, k_y was set equal to x, implying a complete reliance of the predator on the prey population for its sustenance and survival. Following the aforementioned assumptions and relations, model (1) can be articulated as:

$$\begin{aligned} \frac{dx}{dt} &= rx\left(1-\frac{x}{k}\right) - \frac{axy}{1+ahx} - j\left(1-e^{-y}\right)x, \\ \frac{dy}{dt} &= \frac{eaxy}{1+ahx} - \frac{eay^2}{1+ahx} - uy - m(1+\cos(x))y, \end{aligned} \tag{2}$$

where the components of the model (2) are illustrated in the following Table 1.

Furthermore, the term $j\left(1-e^{-y}\right)x$ denotes the rate of change in the prey population arising from its interaction with predators influenced by the predation skill augmentation effect. Concurrently, the term $m(1+\cox(x))y$ signifies the rate of change in the predator population stemming from its interaction with the portion of prey affected by the Hide-and-Escape effect.

3. Boundedness and positivity

Before delving into the detailed analysis of the prey–predator system, it is crucial to establish the concept of boundedness. Boundedness guarantees that the populations of both the prey and predator species do not exceed certain limits determined by ecological factors such as resource availability, predation rates, and carrying capacities.

Theorem 1. *The solutions of system (2) in $\mathbb{R}^2_+$ are bounded as well as invariant positively.*

Proof. In system (2), the equation of the prey is bounded according to the autonomous logistic growth model

$$\frac{dx(t)}{dt} = rx(t)\left(1 - \frac{x(t)}{k}\right),$$

where its solution is,

$$x(t) = \frac{kx(0)}{(k - x(0))e^{-rt} + x(0)}.$$

Having $x < k$, for all $t > 0$, this indicates that the prey equation in system (2) is bounded $\frac{dx}{dt} < rx\left(1 - \frac{x}{k}\right)$ since $\frac{axy}{1+ahx}$ and $j\,(1 - e^{-y})\,x$ are non-positive.

Now, let

$$E(t) = x(t) + y(t).$$

Then the derivative of $E(t)$ is

$$\frac{dE}{dt} = \frac{dx}{dt} + \frac{dy}{dt}. \tag{3}$$

By substituting system (2) in Eq. (3), the following is obtained

$$\begin{aligned}\frac{dE}{dt} =& rx\left(1 - \frac{x}{k}\right) - \frac{axy}{1+ahx} - j\,(1 - e^{-y})\,x \\ &+ \frac{eaxy}{1+ahx} - \frac{eay^2}{1+ahx} - uy - m(1 + \cos(x))y.\end{aligned} \tag{4}$$

The maximum of the term $rx\left(1 - \frac{x}{k}\right)$ can be found by sitting $rx\left(1 - \frac{x}{k}\right) = 0$. Taking the derivative leads to $x = \frac{k}{2}$, which indicates

$$\max\left(rx\left(1 - \frac{x}{k}\right)\right) = \left(r\frac{k}{2}\left(1 - \frac{\frac{k}{2}}{k}\right)\right) = \frac{rk}{4}.$$

Thus, Eq. (4) can be written as follows:

$$\frac{dE}{dt} \le \frac{rk}{4} + \frac{eaxy}{1+ahx} - \frac{eay^2}{1+ahx} - uy - m(1 + \cos(x))y + E - E,$$

$$\frac{dE}{dt} + E \le \frac{rk}{4} + x + y + \frac{eaxy}{1+ahx} - \frac{eay^2}{1+ahx} - uy - m(1 + \cos(x))y. \tag{5}$$

Since $x < k$ for all $t > 0$, Eq. (5) can be written as

$$\frac{dE}{dt} + E \le \frac{rk}{4} + k + y + \frac{eaky}{1+ahk} - \frac{eay^2}{1+ahk} - uy - m(1 + \cos(k))y. \tag{6}$$

Similarly, the maximum value of

$$\left(y + \frac{eaky}{1+ahk} - \frac{eay^2}{1+ahk} - uy - m(1 + \cox(k))y\right)$$

can be found by the following sitting:

$$\left(1 + \frac{eak}{1+ahk} - u - m(1 + \cos(k))\right)y - \frac{eay^2}{1+ahk} = 0.$$

Consequently,

$$y = \frac{\left(1 + \frac{eak}{1+ahk} - u - m(1 + \cos(k))\right)(1 + ahk)}{2ea}.$$

Thus,

$$\frac{dE}{dt} + E \le P, \tag{7}$$

where

$$P = \frac{rk}{4} + k + \left(1 + \frac{eak}{1+ahk} - u - m(1+\cos(k))\right) S - \frac{eaS^2}{1+ahk},$$

and

$$S = \frac{\left(1 + \frac{eak}{1+ahk} - u - m(1+\cos(k))\right)(1+ahk)}{2ea}.$$

Now, simplifying Eq. (7) to obtain

$$\frac{dE}{P-E} \leq dt. \tag{8}$$

To find $E(t)$, integrating both sides of Eq. (8) as follows:

$$-\ln(P-E) \leq t + c,$$
$$\frac{1}{(P-E)} \leq e^{t+c},$$
$$\frac{1}{e^{t+c}} \leq P - E,$$
$$E \leq P - \frac{1}{e^{t+c'}},$$
$$E \leq P + \alpha e^{-t},$$

where $\alpha = \frac{-1}{e^c}$.

Thus

$$E \leq P,$$

when t approach to ∞, which means the system is bounded. Consequently, the system is positively invariant. □

4. Equilibrium points and stability analysis

In this section, equilibrium points, local stability, and global stability of the system (2) will be studied.

4.1. Equilibrium points

Through analysis, it has been determined that the system possesses four equilibrium points, which are obtained by assuming $\frac{dx}{dt} = \frac{dy}{dt} = 0$, in system (2). The equilibrium points within the system (2) are attained in the following manner: - Set $x, y = 0$ then the trivial equilibrium point is $E^1 = (0,0)$

- Assume $x = 0$ then the following formula will be obtained:

$$y(-eay - (u+m)) = 0.$$

When $y = 0$, this leads to a trivial solution or

$$-eay - (u+m) = 0.$$

Then,

$$y = -\frac{u+m}{ea}.$$

This indicates that $E^2 = \left(0, -\frac{u+m}{ea}\right)$. The predator-only equilibrium point will be overlooked or disregarded due to its negative nature according to ecological limitations.

- Assume that $y = 0$, then

$$rx\left(1 - \frac{x}{k}\right) - \frac{ax(0)}{1+ahx} - j\left(1 - e^{-(0)}\right)x = 0,$$

which leads to

$$rx\left(1 - \frac{x}{k}\right) = 0.$$

Then, either $rx = 0$, which implies $x = 0$, or $\left(1 - \frac{x}{k}\right) = 0$, which leads to get $x = k$. Then, the prey-only equilibrium point is $E^3 = (k, 0)$, which is positive without any condition.

- For the fourth equilibrium point (coexistence point),

$$r\left(1-\frac{x}{k}\right)-\frac{ay}{1+ahx}-j\left(1-e^{-y}\right)=0, \tag{9}$$

$$\frac{eax}{1+ahx}-\frac{eay}{1+ahx}-u-m(1+\cos(x))=0. \tag{10}$$

Since $j\left(1-e^{-y}\right)$ in the first quarter is bounded by $[0,j]$, and $m(1+\cos(x))$ lies in $[0,2m]$, Eqs. (9) and (10) can be written as follow:

$$r\left(1-\frac{x}{k}\right)-\frac{ay}{1+ahx}-\gamma=0, \tag{11}$$

$$\frac{eax}{1+ahx}-\frac{eay}{1+ahx}-u-\delta=0, \tag{12}$$

where

$$\gamma=j\left(1-e^{-y}\right)\in[0,j], \tag{13}$$

$$\delta=m(1+\cos(x))\in[0,2m]. \tag{14}$$

From Eq. (11),

$$\frac{a}{1+ahx}y=r\left(1-\frac{x}{k}\right)-\gamma.$$

Thus,

$$y=\frac{1+ahx}{a}\left(r\left(1-\frac{x}{k}\right)-\gamma\right). \tag{15}$$

By substituting Eq. (15) into Eq. (12), the following result can be obtained,

$$\begin{aligned}
\frac{eax}{1+ahx}-\frac{ea}{1+ahx}\frac{1+ahx}{a}\left(r\left(1-\frac{x}{k}\right)-\gamma\right)-u-\delta&=0,\\
\frac{eax}{1+ahx}-e\left(r\left(1-\frac{x}{k}\right)-\gamma\right)-u-\delta&=0,\\
eax-(1+ahx)e\left(r\left(1-\frac{x}{k}\right)-\gamma\right)-(1+ahx)(u+\delta)&=0,\\
eax-(1+ahx)er+(1+ahx)\frac{er}{k}x+(1+ahx)e\gamma-(1+ahx)(u+\delta)&=0,\\
eax-er-erahx+\frac{er}{k}x+\frac{erah}{k}x^2+e\gamma+e\gamma ahx-(u+\delta)-(u+\delta)ahx&=0,\\
\left[\frac{erah}{k}\right]x^2+\left[ea-erah+\frac{er}{k}+e\gamma ah-(u+\delta)ah\right]x+[e\gamma-er-(u+\delta)]&=0.
\end{aligned}$$

In the current case, the determination of the value of x poses a challenge, thus necessitating the demonstration of the existence of at least one positive root for the equation.

The root of previous quadratic equation can be found as follow, if $a_1x^2+a_2x+a_3=0$ be a quadratic equation then the roots $x_{1,2}=\frac{-a_2\mp\sqrt{(a_2)^2-4a_1a_3}}{2a_1}$, if $D=\left((a_2)^2-4a_1a_3\right)>0$, and $a_3<0$, that means the equation have at least one positive root.

Now, $a_3=e\gamma-er-(u+\delta)<0$, if $\gamma<r$, which is true always since in this system it was assumed that the growth rate of prey r is bigger than the parameter j. Thus, $-4a_1a_3$, is non-negative.

On the other hand, the term $\left[ea-erah+\frac{er}{k}+e\gamma ah-(u+\delta)ah\right]^2$, is always positive which is led to conclude that $D>0$, that means there is at least one positive root say $\bar{x}$, to get the value of y substituting $\bar{x}$ in Eq. (15),

$$\bar{y}=\frac{1+ahx}{a}\left(r\left(1-\frac{\bar{x}}{k}\right)-\gamma\right)>0.$$

Consequently, $\bar{y}$ is always positive since $r\left(1-\frac{\bar{x}}{k}\right)>\gamma$. Therefore, $E^4=(\bar{x},\bar{y})$, is always positive.

4.2. Local stability

The local stability of an equilibrium points in a prey–predator system can be examined using various methods. This subsection will examine two frequently employed methodologies: the eigenvalues method and the trace-determinant method. These methodologies offer significant insights into the stability characteristics of the system through the analysis of the eigenvalues of the Jacobian matrix and the assessment of the matrix's trace and determinant. Through the utilization of these methodologies, it is possible to evaluate the stability of the equilibrium points and acquire a more profound comprehension of the localized dynamics within the prey–predator system. The Jacobian matrix of system (2) can be written as:

$$J=\begin{bmatrix} a_{11} & a_{12}\\ a_{21} & a_{22}\end{bmatrix},$$

where

$$a_{11} = r\left(1-\frac{2x}{k}\right) - \frac{ay}{(1+ahx)^2} - j\left(1-e^{-y}\right),$$
$$a_{12} = -\frac{ax}{1+ahx} - je^{-y}x,$$
$$a_{21} = \frac{eay}{(1+ahx)^2} + \frac{ea^2hy^2}{(1+ahx)^2} + my\sin(x),$$
$$a_{22} = \frac{ea(x-2y)}{1+ahx} - u - m(1+\cos(x)).$$

The subsequent theorems will address the issue of local stability pertaining to the positive points of system (2).

Theorem 2. *The trivial equilibrium point $E^1(0,0)$ is unstable saddle–node in system (2).*

Proof. Consider the Jacobian matrix of system (2) on $E^1(0,0)$,

$$JE^1 = \begin{bmatrix} r & 0 \\ 0 & -u-2m \end{bmatrix}.$$

By a direct calculation of the eigenvalues $\lambda_1 = r > 0$, and $\lambda_2 = -(u+m) < 0$, E^1 is unstable saddle point. □

Theorem 3. *If $\frac{eak}{1+ahk} < u + m(1+\cos(k))$, in system (2) then $E^3(k,0)$, is local asymptotically stable.*

Proof. Consider the Jacobian matrix on prey-only equilibrium point $E^3 = (k,0)$,

$$JE^3(k,0) = \begin{bmatrix} -r & -\frac{ak}{1+ahk} - jk \\ 0 & \frac{eak}{1+ahk} - u - m(1+\cos(k)) \end{bmatrix}.$$

By a direct calculation, it can be determined that the eigenvalues of the system are,

$$\lambda_1 = -r < 0,$$

and

$$\lambda_2 = \frac{eak}{1+ahk} - u - m(1+\cos(k)).$$

Consequently, it can be concluded that $E^3(k,0)$, is local asymptotically stable if

$$\frac{eak}{1+ahk} < u + m(1+\cos(k)). \quad \square$$

Theorem 4. *$E^4 = (\bar{x},\bar{y})$, is local asymptotically stable if*

$$\bar{x} > \frac{k}{2}. \tag{16}$$

and

$$\bar{x} < 2\bar{y}. \tag{17}$$

Proof. Consider the Jacobian matrix that evaluated at the coexistence equilibrium point $E^4 = (\bar{x},\bar{y})$

$$JE^4 = \begin{bmatrix} r\left(1-\frac{2\bar{x}}{k}\right) - \frac{a\bar{y}}{(1+ah\bar{x})^2} - j\left(1-e^{-\bar{y}}\right) & -\frac{a\bar{x}}{1+ah\bar{x}} - je^{-\bar{y}}\bar{x} \\ \frac{ea\bar{y}(1+ah\bar{y})}{(1+ah\bar{x})^2} + m\bar{y}\sin(\bar{x}) & \frac{ea(\bar{x}-2\bar{y})}{1+ah\bar{x}} - u - m(1+\cos(\bar{x})) \end{bmatrix}.$$

The determinant of JE^4 is

$$\begin{aligned}\det\left(JE^4\right) =& r\left(1-\frac{2\bar{x}}{k}\right)\frac{ea(\bar{x}-2\bar{y})}{1+ah\bar{x}} - ur\left(1-\frac{2\bar{x}}{k}\right) - mr\left(1-\frac{2\bar{x}}{k}\right)(1+\cos(\bar{x})) - \frac{ea^2\bar{y}(\bar{x}-2\bar{y})}{(1+ah\bar{x})^3} + \frac{au\bar{y}}{(1+ah\bar{x})^2} \\ &+ \frac{am\bar{y}(1+\cos(\bar{x}))}{(1+ah\bar{x})^2} - \frac{ea(\bar{x}-2\bar{y})j\left(1-e^{-\bar{y}}\right)}{1+ah\bar{x}} + ju\left(1-e^{-\bar{y}}\right) + jm\left(1-e^{-\bar{y}}\right)(1+\cos(\bar{x})) \\ &+ \left(\frac{ea\bar{y}(1+ah\bar{y})}{(1+ah\bar{x})^2} + m\bar{y}\sin(\bar{x})\right)\left(\frac{a\bar{x}}{1+ah\bar{x}} + je^{-\bar{y}}\bar{x}\right),\end{aligned}$$

which is positive if $\bar{x} > \frac{k}{2}$, and $2\bar{y} > \bar{x}$.

On the other hand, the trace of JE^4 is

$$\text{trace}\left(JE^4\right) = r\left(1-\frac{2\bar{x}}{k}\right) - \frac{a\bar{y}}{(1+ah\bar{x})^2} - j\left(1-e^{-\bar{y}}\right) + \frac{ea(\bar{x}-2\bar{y})}{1+ah\bar{x}} - u - m(1+\cos(\bar{x})),$$

which is negative under the same conditions, then E^4 is local asymptotically stable. □

4.3. Global stability analysis

The analysis of global stability in prey–predator systems holds significant importance in understanding the persistent dynamics and ecological implications of the interactions between prey and predator. Through analyzing the concept of global stability, it is possible to determine the ability of a system to achieve a state of stable equilibrium regardless of its initial conditions. The present analysis provides significant insights into the persistent and resilient dynamics that exist between prey and predator. The examination of the global stability of the system (2) has been conducted through the utilization of the Dulac criterion and the Poincare–Bendixson theorem.

Theorem 5. *System (2) has no periodic solution then it is globally stable on E^4 if the condition (16) is satisfied.*

Proof. Define a Dulac function $H = \frac{1+ahx}{xy}$, which is continuously differentiable within $\mathbb{R}^2_+$. Let $N^1 = \frac{dx}{dt}$, and $N^2 = \frac{dy}{dt}$, in system (2). By multiplying H by N^1 yields:

$$HN^1 = \left(rx\left(1-\frac{x}{k}\right) - \frac{axy}{1+ahx} - j\left(1-e^{-y}\right)x\right)\frac{1+ahx}{xy}. \tag{18}$$

By applying the partial derivative to both sides of Eq. (18) with respect to x, the following expression can be derived,

$$\begin{aligned}\frac{\partial HN^1}{\partial x} &= \frac{e^{-y}ahjk - ahjk + ahkr - 2ahrx - r}{ky},\\ &= \frac{-ahjk\left(1-e^{-y}\right) - ahk(2x-k) - r}{ky}.\end{aligned}$$

On the other hand, multiplying H by N^2 yields:

$$\begin{aligned}HN^2 &= \left(\frac{eaxy}{1+ahx} - \frac{eay^2}{1+ahx} - uy - m(1+\cos(x))y\right)\frac{1+ahx}{xy}\\ &= ea - \frac{eay}{x} - \frac{u(1+ahx)}{x} - \frac{m(1+\cos(x))(1+ahx)}{x}.\end{aligned} \tag{19}$$

Also, by taking the partial derivative to both sides of Eq. (19) with respect to y, the following is obtained,

$$\frac{\partial HN^2}{\partial y} = -\frac{ea}{x}.$$

Therefore,

$$\frac{\partial HN^1}{\partial x} + \frac{\partial HN^2}{\partial x} = \frac{-ahj\left(1-e^{-y}\right)}{y} - \frac{ahk(2x-k)}{ky} - \frac{r}{ky} - \frac{ea}{x}.$$

If condition (16) is satisfied, it can be concluded that $\frac{\partial HN^1}{\partial x} + \frac{\partial HN^2}{\partial y} < 0$, which means that by Dulac criterion the system has no periodic solution. Consequently, depending on the Poincare–Bendixson theorem, E^4 is a global stabile.

It is noteworthy that the presence of a similarity between the condition for global stability and the condition for local stability at the point of coexistence serves as an indication of the analytical accuracy and validity of the condition. □

5. Kolmogorov analysis

The utilization of Kolmogorov analysis is a potent methodology employed to investigate the factors that contribute to the persistence and extinction phenomena in prey–predator systems existing in two-dimensional environments. The utilization of Kolmogorov conditions enables us to investigate the enduring dynamics and population phenomena exhibited by species that interact with one another. This analysis enables the identification of crucial parameters and thresholds that govern the long-term survival or extinction of prey or predator populations. Gaining a comprehensive understanding of the Kolmogorov conditions offers valuable insights into the long-time behavior of prey–predator systems, thereby facilitating ecological management and conservation endeavors.

System (2) if $\frac{dx}{dt} = xM^1(x,y)$ and $\frac{dy}{dt} = yM^2(x,y)$ can be written as follow:

$$\begin{aligned}xM^1(x,y) &= x\left(r\left(1-\frac{x}{k}\right) - \frac{ay}{1+ahx} - j\left(1-e^{-y}\right)\right),\\ yM^2(x,y) &= y\left(\frac{eax}{1+ahx} - \frac{eay}{1+ahx} - u - m(1+\cos(x))\right),\end{aligned} \tag{20}$$

where $M^1(x,y)$, and $M^2(x,y)$, are denote to the growth rates of the species, which are associated with the current density of prey x, and predator y.

Theorem 6. *If the population of prey remains fixed while the population of predators increases, it can be expected that the growth rates of both predators and prey will decline.*

Proof. According to Kolmogorov by assuming the prey number fixed and differentiating system (20) with respect to y, the result can be acquired,

$$\frac{\partial M^1}{\partial y} = -\frac{a}{1+ahx} - e^{-y} < 0,$$
$$\frac{\partial M^2}{\partial y} = -\frac{ea}{1+ahx} < 0.$$

Since $\frac{\partial M^1}{\partial y}$ and $\frac{\partial M^2}{\partial y}$ are negative, this implies that the growth rate of both species will decrease according to [31]. □

Theorem 7. *The minimum carrying capacity that required to support the growth of prey is k.*

Proof. Assume that there is $P > 0$, such that $M^1(P, 0) = 0$. Then, $r\left(1 - \frac{P}{k}\right) = 0$. Consequently, $P = k$. Which is the least carrying capacity that required to support the growth of prey. □

Theorem 8. *The minimum number of preys that required to sustain the predator population at its lowest growth rate within the system is*

$$\omega = \frac{u+\delta}{ea - ah\delta - ahu}.$$

Proof. Let $\omega > 0$, be the least number of prey. Then,

$$M^2(\omega, 0) = \frac{ea\omega}{1+ah\omega} - u - m(1+\cos(\omega)).$$

According to (14),

$$\delta = m(1+\cos(\omega)),$$

which leads to

$$M^2(\omega, 0) = \frac{ea\omega}{1+ah\omega} - u - \delta = 0,$$
$$ea\omega = u(1+ah\omega) + \delta(1+ah\omega),$$
$$ea\omega = u + ahu\omega + \delta + ah\delta\omega,$$
$$(ea - ah\delta - ahu)\omega = u + \delta,$$

and consequently

$$\omega = \frac{u+\delta}{ea - ah\delta - ahu}$$

is the least number of preys that required to keep the predator population at its lowest growth rate. □

Theorem 9. *In system (20), the prey and predator exhibit coexistence if*

$$k > \frac{u+\delta}{ea - ah\delta - ahu}.$$

Proof. According to Kolmogorov, the persistence of an ecosystem is contingent upon the condition where the carrying capacity of the prey population exceeds the minimum number of prey required to sustain the predator population at its lowest growth rate [31]. This implies that the prey and predator are coexist if $P > \omega$, and

$$k > \frac{u+\delta}{ea - ah\delta - ahu}. \tag{21}$$

Condition (21), in turn, will result in a rise in the population of prey and, correspondingly, an increase in the population of predators. □

6. Local bifurcation

The analysis of bifurcations in prey–predator systems provides valuable insights into the intricate dynamics and behaviors manifested by ecological interactions. The analysis of bifurcation offers a more profound comprehension of how alterations in parameters can result in qualitative transformations in the dynamics of a population, such as the occurrence of oscillations, stable coexistence, or sudden transitions. Through the examination of bifurcations, crucial thresholds and tipping points can be discerned that exert an impact on the stability and longevity of various species. The acquisition of this knowledge is imperative in order to make accurate predictions and effectively manage ecological systems. It allows us to evaluate the consequences of disturbances and devise efficient approaches for the preservation and sustainable management of ecosystems. The local bifurcation in this section is studied using "Sotomayor theorem" [31].

Consider the dynamical system that can be described by the vector field $F(x, y, \mu^*) = 0$, where $DF = J$, has a zero eigenvalue, with eigenvector ξ^n, and J^T, has a zero eigenvalue, with eigenvector φ^m. Then the following are satisfied, the system has:

Saddle–node bifurcation if,

- $\varphi^{mT} F_{\mu}(E^*, \mu^*) \neq 0$,
- $\varphi^{mT}\left(D^2 F(E^*, \mu^*)\xi^n\right) \neq 0$.

Trans-critical bifurcation if,

- $\varphi^{mT} F_{\mu}(E^*, \mu^*) = 0$,
- $\varphi^{mT}\left(DF_{\mu}(E^*, \mu^*)\xi^n\right) \neq 0$,
- $\varphi^{mT}\left(D^2 F(E^*, \mu^*)\xi^n\right) \neq 0$.

Pitchfork bifurcation if,

- $\varphi^{mT} F_{\mu}(E^*, \mu^*) = 0$,
- $\varphi^{mT}\left(DF_{\mu}(E^*, \mu^*)\xi^n\right) \neq 0$,
- $\varphi^{mT}\left(D^2 F(E^*, \mu^*)\xi^n\right) = 0$,
- $\varphi^{mT}\left(D^3 F(E^*, \mu^*)\xi^n\right) \neq 0$.

For this purpose, system (2) can be written by the vector F as follow:

$$F = \begin{bmatrix} x\left(r\left(1-\frac{x}{k}\right) - \frac{ay}{1+ahx} - j\left(1-e^{-y}\right)\right) \\ y\left(\frac{eax}{1+ahx} - \frac{eay}{1+ahx} - u - m(1+\cos(x))\right) \end{bmatrix}.$$

Let $\xi^n = \begin{bmatrix} \xi^n_{(1)} & \xi^n_{(2)} \end{bmatrix}^T$ be any eigenvector then,

$$DF\xi^n = \begin{bmatrix} \left(r\left(1-\frac{2x}{k}\right) - \frac{ay}{(1+ahx)^2} - j\left(1-e^{-y}\right)\right)\xi^n_{(1)} + \left(-\frac{ax}{1+ahx} - je^{-y}x\right)\xi^n_{(2)} \\ \left(\frac{eay(1+ahy)}{(1+ahx)^2} + my\sin(x)\right)\xi^n_{(1)} + \left(\frac{ea(x-2y)}{1+ahx} - u - m(1+\cos(x))\right)\xi^n_{(2)} \end{bmatrix}.$$

Let $DF\xi^n = \begin{bmatrix} T_1 \\ T_2 \end{bmatrix}$, then

$$D^2 F\xi^n = \begin{bmatrix} \frac{\partial T_1}{\partial x} & \frac{\partial T_1}{\partial y} \\ \frac{\partial T_2}{\partial x} & \frac{\partial T_2}{\partial y} \end{bmatrix}\begin{bmatrix} \xi^n_{(1)} \\ \xi^n_{(2)} \end{bmatrix} = \begin{bmatrix} \xi^n_{(1)}\frac{\partial T_1}{\partial x} + \xi^n_{(2)}\frac{\partial T_1}{\partial y} \\ \xi^n_{(1)}\frac{\partial T_2}{\partial x} + \xi^n_{(2)}\frac{\partial T_2}{\partial y} \end{bmatrix} = \begin{bmatrix} R_1 \\ R_2 \end{bmatrix}.$$

where

$$\frac{\partial T_1}{\partial x} = \left(\frac{2r}{k} + \frac{2a^2hy}{(1+ahx)^3}\right)\xi^n_{(1)} + \left(\frac{a^2hx}{(1+ahx)^2} - \frac{a}{1+ahx} - je^{-y}\right)\xi^n_{(2)},$$
$$\frac{\partial T_1}{\partial y} = \left(\frac{-a}{(1+ahx)^2} - je^{-y}\right)\xi^n_{(1)} + je^{-y}x\xi^n_{(2)},$$
$$\frac{\partial T_2}{\partial x} = \left(\frac{-2ea^2hy(1+ahy)}{(1+ahx)^3} + my\cos(x)\right)\xi^n_{(1)} + \left(\frac{ea(1+2ahy)}{(1+ahx)^2} + m\sin(x)\right)\xi^n_{(2)},$$
$$\frac{\partial T_2}{\partial y} = \left(\frac{ea(1+2ahy)}{(1+ahx)^2} + m\sin(x)\right)\xi^n_{(1)} - \frac{2ea}{1+ahx}\xi^n_{(2)},$$

and,

$$R_1 = \left(\left(\frac{2r}{k} + \frac{2a^2hy}{(1+ahx)^3}\right)\xi^n_{(1)} + \left(\frac{a^2hx}{(1+ahx)^2} - \frac{a}{1+ahx} - je^{-y}\right)\xi^n_{(2)}\right)\xi^n_{(1)}$$
$$+ \left(\left(\frac{-a}{(1+ahx)^2} - je^{-y}\right)\xi^n_{(1)} + je^{-y}x\xi^n_{(2)}\right)\xi^n_{(2)},$$
$$R_2 = \left(\left(\frac{-2ea^2hy(1+ahy)}{(1+ahx)^3} + my\cos(x)\right)\xi^n_{(1)} + \left(\frac{ea(1+2ahy)}{(1+ahx)^2} + m\sin(x)\right)\xi^n_{(2)}\right)\xi^n_{(1)}$$
$$+ \left(\left(\frac{ea(1+2ahy)}{(1+ahx)^2} + m\sin(x)\right)\xi^n_{(1)} - \frac{2ea}{1+ahx}\xi^n_{(2)}\right)\xi^n_{(2)}.$$

Similarly, $D^3 F\xi^n$ can be found as

$$D^3 F\xi^n = \begin{bmatrix} \frac{\partial R_1}{\partial x} & \frac{\partial R_1}{\partial y} \\ \frac{\partial R_2}{\partial x} & \frac{\partial R_2}{\partial y} \end{bmatrix}\begin{bmatrix} \xi^n_{(1)} \\ \xi^n_{(2)} \end{bmatrix} = \begin{bmatrix} \xi^n_{(1)}\frac{\partial R_1}{\partial x} + \xi^n_{(2)} & \frac{\partial R_1}{\partial y} \\ \xi^n_{(1)}\frac{\partial R_2}{\partial x} + \xi^n_{(2)}\big) & \frac{\partial R_2}{\partial y} \end{bmatrix} = \begin{bmatrix} R_3 \\ R_4 \end{bmatrix},$$

where

$$R_3 = \xi^n_{(1)}\frac{\partial R_1}{\partial x} + \xi^n_{(2)}\frac{\partial R_1}{\partial y},$$

and

$$R_4 = \xi^n_{(1)} \frac{\partial R_2}{\partial x} + \xi^n_{(2)} \frac{\partial R_2}{\partial y}.$$

Theorem 10. *For the parameter*

$$u^* = \frac{eak}{1+ahk} - m(1+\cox(k)),$$

with $E^3(k,0)$*, system* (2) *has:*

- *No saddle–node bifurcation,*
- *Trans-critical bifurcation,*
- *Pitchfork bifurcation if*

$$\left(\frac{ea}{(1+ahk)^2} + m\sin(k)\right)\left(\frac{-ak}{r(1+ahk)} - \frac{jk}{r}\right) = \frac{ea}{1+ahk'},$$

and

$$\left[\frac{6ea^3h^2y}{(1+ahx)^4} + \frac{6ea^4h^3y^2}{(1+ahx)^4} - my\sin(x)\right]\left(\frac{-ak}{r(1+ahk)} - \frac{jk}{r}\right)^2 + \frac{6ea^2h}{(1+ahx)^2} \neq \left[\frac{6ea^2h}{(1+ahx)^3} + \frac{12ea^3h^2y}{(1+ahx)^3} - 3m\cos(x)\right]\left(\frac{-ak}{r(1+ahk)} - \frac{jk}{r}\right).$$

Proof. Suppose that

$$u = \frac{eak}{1+ahk} - m(1+\cos(k)) = u^*$$

is the Jacobian matrix which can be written as follow:

$$J^*E^3(k,0) = \begin{bmatrix} -r & -\frac{ak}{1+ahk} - jk \\ 0 & 0 \end{bmatrix}.$$

Since, $\lambda_{31} = -r < 0$, and $\lambda_{32} = 0$. Then, $E^3(k,0)$, becomes a non-hyperbolic point. Let $\xi^1 = \begin{bmatrix} \xi^1_{(1)} & \xi^1_{(2)} \end{bmatrix}^T$, be the corresponding eigenvector to $\lambda_{32} = 0$, then, $\left(J^*E^3(k,0) - \lambda_{32}I\right)\xi^1 = 0$.

By a direct calculation if $\xi^1_{(2)} = 1$, this yields

$$\xi^1 = \begin{bmatrix} \frac{-ak}{r(1+ahk)} - \frac{jk}{r} & 1 \end{bmatrix}^T.$$

To compute $\varphi^1 = \begin{bmatrix} \varphi^1_{(1)} & \varphi^1_{(2)} \end{bmatrix}^T$, which is the corresponding eigenvector of $\left[J^*E^3(k,0)\right]^T$, let

$$\left(\left[J^*E^3(k,0)\right]^T - \lambda_{32}I\right)\varphi^1 = 0,$$

where

$$\left[J^*E^3(k,0)\right]^T = \begin{bmatrix} -r & 0 \\ -\frac{ak}{1+ahk} - jk & 0 \end{bmatrix},$$

and

$$\varphi^1 = \begin{bmatrix} \varphi^1_{(1)} & \varphi^1_{(2)} \end{bmatrix}^T.$$

Thus,

$$\left[J^*E^3(k,0)\right]^T\varphi^1 = \begin{bmatrix} -r & 0 \\ -\frac{ak}{1+ahk} - jk & 0 \end{bmatrix}\begin{bmatrix} \varphi^1_{(1)} \\ \varphi^1_{(2)} \end{bmatrix} = \begin{bmatrix} 0 \\ 0 \end{bmatrix},$$

$$\left[\left(-\frac{ak}{-r\varphi^1_{(1)}} - jk\right)\varphi^1_{(1)}\right] = \begin{bmatrix} 0 \\ 0 \end{bmatrix}.$$

Since $-r$ and $-\frac{ak}{1+ahk} - jk$ are not equal to zero, this indicates that $\varphi^1_{(1)} = 0$, with $\varphi^1_{(2)} \neq 0$. Assuming that $\varphi^1_{(2)}$ be any non-zero value, then

$$\varphi^1 = \begin{bmatrix} 0 & 1 \end{bmatrix}^T.$$

Taking the derivative of F with respect to u, yields,

$$F_u = \begin{bmatrix} 0 \\ -y \end{bmatrix},$$

and

$$F_u\left(E^3,u^*\right)=\begin{bmatrix}0\\0\end{bmatrix}.$$

Thus,

$$\varphi^{1^T}F_u\left(E^3,u^*\right)=\begin{bmatrix}0 & 1\end{bmatrix}\begin{bmatrix}0\\0\end{bmatrix}=0.$$

Consequently, the first condition on trans-critical bifurcation occurs. Since $\varphi^{1^T}F_u\left(E^3,u^*\right)=0$, the saddle–node bifurcation cannot occur. Moreover, finding the second condition can be done as follows:

$$DF_u\left(E^3,u^*\right)\xi^1=\begin{bmatrix}0 & 0\\0 & -1\end{bmatrix}\begin{bmatrix}\frac{-ak}{r(1+ahk)}-\frac{jk}{r}\\1\end{bmatrix}=\begin{bmatrix}0\\-1\end{bmatrix},$$

$$\varphi^{1^T}\left(DF_u\left(E^3,u\right)\xi^1\right)=\begin{bmatrix}0 & 1\end{bmatrix}\begin{bmatrix}0\\-1\end{bmatrix}=-1\neq 0,$$

which is the second condition of trans-critical bifurcation.

Computing the third condition can be done by substituting $x=k, y=0, \xi^1_{(1)}=\frac{-ak}{r(1+ahk)}-\frac{jk}{r}$, and $\xi^1_{(2)}=1$ in $D^2F\left(E^3,u\right)\xi^n$, where $n=1$, and multiplying it by φ^{1^T} to obtain

$$\varphi^{1^T}\left(D^2F\left(E^3,u\right)\xi^1\right)=\begin{bmatrix}0 & 1\end{bmatrix}\begin{bmatrix}\xi^1_{(1)}\frac{\partial T_1}{\partial x}+\xi^1_{(2)}\frac{\partial T_1}{\partial y}\\ \xi^1_{(1)}\frac{\partial T_2}{\partial x}+\xi^1_{(2)}\frac{\partial T_2}{\partial y}\end{bmatrix},$$

$$\varphi^{1^T}\left(D^2F\left(E^3,u\right)\xi^1\right)=2\left(\frac{ea}{(1+ahx)^2}+m\sin(x)\right)\left(\frac{-ak}{r(1+ahk)}-\frac{jk}{r}\right)-\frac{2ea}{1+ahx}\neq 0.$$

By Sotomayor theorem for local bifurcation, the system has trans-critical bifurcation at $E^3(k,0)$, when $u^*=\frac{eak}{1+ahk}-m(1+\cos(k))$. Consequently, if

$$\left(\frac{ea}{(1+ahk)^2}+m\sin(k)\right)\left(\frac{-ak}{r(1+ahk)}-\frac{jk}{r}\right)=\frac{ea}{1+ahk},\tag{22}$$

then there is a possibility of pitchfork bifurcation occurring.

Suppose that condition (22) holds, then the fourth condition of pitchfork bifurcation must be obtained. The value of $\varphi^{1^T}D^3F\xi^1$ can be found by,

$$\varphi^{1^T}\left(D^3F\left(E^3,u^*\right)\xi^1\right)=\begin{bmatrix}0 & 1\end{bmatrix}\begin{bmatrix}\xi^1_{(1)}\frac{\partial R_1}{\partial x}+\xi^1_{(2)}\frac{\partial R_1}{\partial y}\\ \xi^1_{(1)}\frac{\partial R_2}{\partial x}+\xi^1_{(2)}\frac{\partial R_2}{\partial y}\end{bmatrix},$$

$$\varphi^{1^T}\left(D^3F\left(E^3,u^*\right)\xi^1\right)=\xi^1_{(1)}\frac{\partial R_2}{\partial x}+\xi^1_{(2)}\frac{\partial R_2}{\partial y}.$$

Consequently, it can be concluded that

$$\begin{aligned}\xi^1_{(1)}\frac{\partial R_2}{\partial x}+\xi^1_{(2)}\frac{\partial R_2}{\partial y}=&\left[\frac{6ea^3h^2y}{(1+ahx)^4}+\frac{6ea^4h^3y^2}{(1+ahx)^4}-my\sin(x)\right]\left(\frac{-ak}{r(1+ahk)}-\frac{jk}{r}\right)^3\\&-\left[\frac{6ea^2h}{(1+ahx)^3}+\frac{12ea^3h^2y}{(1+ahx)^3}-3m\cos(x)\right]\left(\frac{-ak}{r(1+ahk)}-\frac{jk}{r}\right)^2\\&+\frac{6ea^2h}{(1+ahx)^2}\left(\frac{-ak}{r(1+ahk)}-\frac{jk}{r}\right),\end{aligned}$$

which implies that $\varphi^{1^T}\left(D^3F\left(E^3,u^*\right)\xi^1\right)\neq 0$, if

$$\begin{aligned}&\left[\frac{6ea^3h^2y}{(1+ahx)^4}+\frac{6ea^4h^3y^2}{(1+ahx)^4}-my\sin(x)\right]\left(\frac{-ak}{r(1+ahk)}-\frac{jk}{r}\right)^2+\frac{6ea^2h}{(1+ahx)^2}\\&\neq\left[\frac{6ea^2h}{(1+ahx)^3}+\frac{12ea^3h^2y}{(1+ahx)^3}-3m\cos(x)\right]\left(\frac{-ak}{r(1+ahk)}-\frac{jk}{r}\right).\end{aligned}$$

□

Theorem 11. *System (2) with $E^4(\bar{x},\bar{y})$, has:*

- *Saddle–node bifurcation,*
- *No trans-critical bifurcation,*
- *No Pitchfork bifurcation,*

where, the parameter

$$u^*=r\left(1-\frac{2\bar{x}}{k}\right)-\frac{a\bar{y}}{(1+ah\bar{x})^2}-j\left(1-e^{-\bar{y}}\right)+\frac{ea(\bar{x}-2\bar{y})}{1+ah\bar{x}}-m(1+\cos(\bar{x})).$$

Proof. The Jacobian matrix of system (2) at $E^4(\bar{x},\bar{y})$ is

$$J E^4 = \begin{bmatrix} r\left(1-\frac{2\bar{x}}{k}\right) - \frac{a\bar{y}}{(1+ah\bar{x})^2} - j\left(1-e^{-\bar{y}}\right) & -\frac{a\bar{x}}{1+ah\bar{x}} - je^{-\bar{y}}\bar{x} \\ \frac{ea\bar{y}(1+ah\bar{y})}{(1+ah\bar{x})^2} + m\bar{y}\sin(\bar{x}) & \frac{ea(\bar{x}-2\bar{y})}{1+ah\bar{x}} - u^* - m(1+\cos(\bar{x})) \end{bmatrix}.$$

Let Det $\left(J^*E^4\right) = 0$. Then, J^*E^4 has the zero eigenvalue $\lambda_{42} = 0$. Thus, $\lambda_{42} = \text{trace}\left(J^*E^4\right)$, which is negative according to the stability conditions at the same point. Therefore, E^4 is non-hyperbolic point, where

$$u = r\left(1-\frac{2\bar{x}}{k}\right) - \frac{a\bar{y}}{(1+ah\bar{x})^2} - j\left(1-e^{-\bar{y}}\right) + \frac{ea(\bar{x}-2\bar{y})}{1+ah\bar{x}} - m(1+\cos(\bar{x})).$$

Let $\xi^2 = \begin{bmatrix} \xi^2_{(1)} & \xi^2_{(2)} \end{bmatrix}^T$, be the corresponding eigenvector to $\lambda_{42} = 0$ for the matrix J^*E^4. Then, by a direct computation of $\left(J^*E^4(k,0) - \lambda_{42}I\right)\xi^2 = 0$,

$$\xi^2 = \begin{bmatrix} \frac{-a_{12}}{a_{11}} \\ 1 \end{bmatrix}.$$

Also, let $\varphi^1 = \begin{bmatrix} \varphi^1_{(1)} & \varphi^1_{(2)} \end{bmatrix}^T$, be the corresponding eigenvector to $\lambda_{42} = 0$, for the matrix $\left[J^*E^4\right]^T$. Then, by a direct computation of $\left(\left[J^*E^4(k,0)\right]^T - \lambda_{42}I\right)\xi^2 = 0$,

$$\varphi^2 = \begin{bmatrix} \frac{-a_{21}}{a_{11}} & 1 \end{bmatrix}^T.$$

Now, to find F_u, F is differentiated with respect to u, from which it can be inferred that,

$$F_u = \begin{bmatrix} 0 \\ -y \end{bmatrix}.$$

Thus,

$$F_u\left(E^4,u^*\right) = \begin{bmatrix} 0 \\ -\bar{y} \end{bmatrix}.$$

Therefore,

$$\varphi^{2^T} F_u\left(E^4,u^*\right) = \begin{bmatrix} \frac{-a_{21}}{a_{11}} & 1 \end{bmatrix}\begin{bmatrix} 0 \\ -\bar{y} \end{bmatrix} = -\bar{y} \neq 0,$$

which is the first condition of saddle–node bifurcation. Also, it can be concluded that the trans-critical and Pitchfork bifurcations cannot be occurred since there is no condition that can be set to make $\varphi^{2T} F_u\left(E^4,u^*\right) = 0$.

Now, verifying the second one can be done by sitting $x = \bar{x}, y = \bar{y}, \xi^2_{(1)} = \frac{-a_{12}}{a_{11}}$, and $\xi^2_{(2)} = 1$, in $D^2F\left(E^3,u^*\right)\xi^n$, where $n = 2$, which gives

$$D^2F\left(E^4,u^*\right)\xi^2 = \begin{bmatrix} R_1 \\ R_2 \end{bmatrix}.$$

Consequently,

$$\varphi^{2^T}\left(D^2F\left(E^4,u\right)\xi^2\right) = \begin{bmatrix} \frac{-a_{21}}{a_{11}} & 1 \end{bmatrix}\begin{bmatrix} R_1 \\ R_2 \end{bmatrix} \neq 0.$$

By Sotomayor theorem for local bifurcation, the system has saddle–node bifurcation at $E^4(\bar{x},\bar{y})$ when

$$u^* = r\left(1-\frac{2\bar{x}}{k}\right) - \frac{a\bar{y}}{(1+ah\bar{x})^2} - j\left(1-e^{-\bar{y}}\right) + \frac{ea(\bar{x}-2\bar{y})}{1+ah\bar{x}} - m(1+\cos(\bar{x})). \quad \square$$

7. Numerical simulations and discussions

In this section, a numerical simulation is conducted to validate the dynamics of the system and gain a deeper comprehension of how altering parameter values affects the dynamical behavior of the system. In order to simulate the dynamic behavior of the system, various initial values were employed, using a computational method on MATLAB platform. In order to obtain a numerical solution for the system, a set of hypothetical parameter values is employed. It is worth noting that alternative sets of parameter values can also be utilized for this purpose. The selection of parameter values was conducted with the aim of ensuring ecological plausibility of the system as illustrated in Table 2.

Under this data set of parameters, the following equilibrium points are obtained:

- Trivial point $(0,0)$.
- Prey-only point $(4,0)$.
- Coexistence point $(2.5273, 1.0967)$.

Table 2
Data set of selected parameters for system (2).

Name	Parameter	Value	Unit
The growth rate of prey	r	3	time^{-1}
Predation rate	a	2.2	time^{-1}
Predator decay rate	u	0.2	time^{-1}
Half-saturation constant	h	0.5	prey $^{\mid}$
Conversion efficiency	e	0.35	dimensionless
Carrying capacity of prey	k	4	individuals perarea
The proportion of predators that are able to gain predation skill	j	0.7	dimensionless
The proportion of preys that had an opportunity to escape away or hide	m	0.5	dimensionless

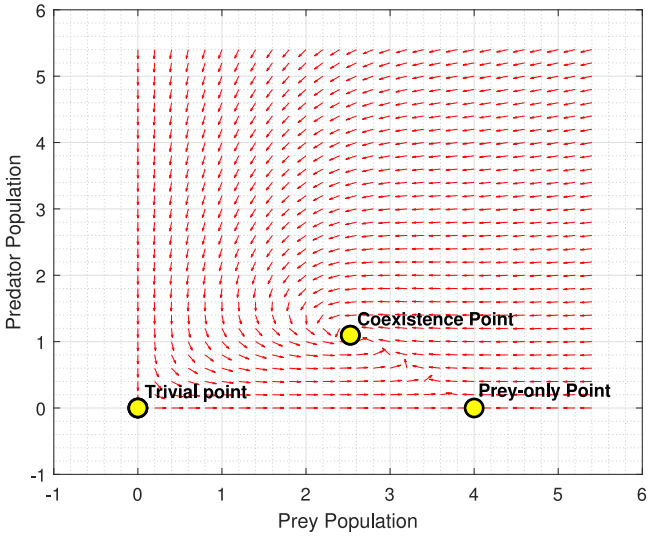

Fig. 3. The equilibrium points of system (2) for the data given in Table 2.

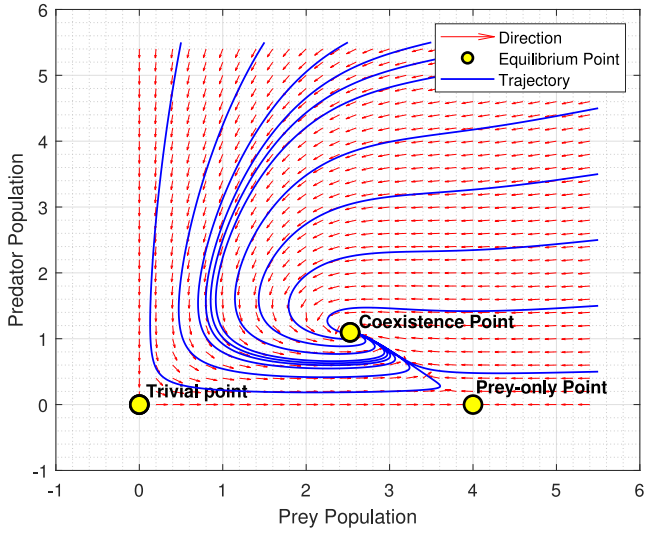

Fig. 4. Phase portrait of system (2) using 11 distinct initial values.

The observed plot of equilibrium points on direction field is illustrated in Fig. 3.

The trajectories of the system were plotted by conducting numerical simulations with 11 distinct initial values as shown in Fig. 4. The distinct initial points were chosen to represent a range of environmental conditions. Five of them were chosen so that the number of prey exceeds the number of predators. This represents the state of prey abundance. The other five points were chosen

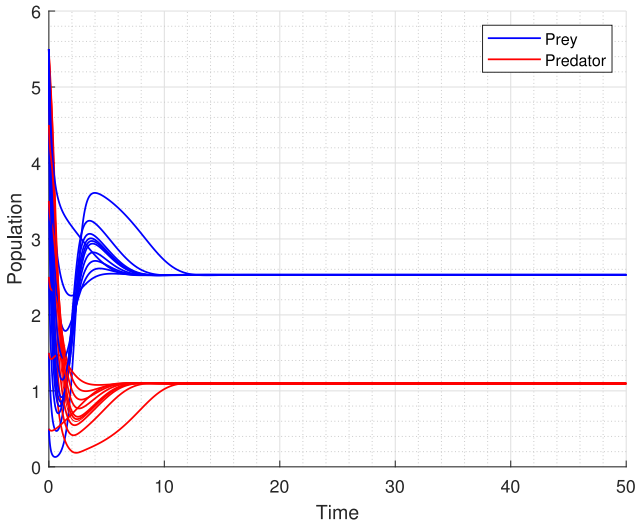

Fig. 5. Time series of system (2) using 11 distinct initial values.

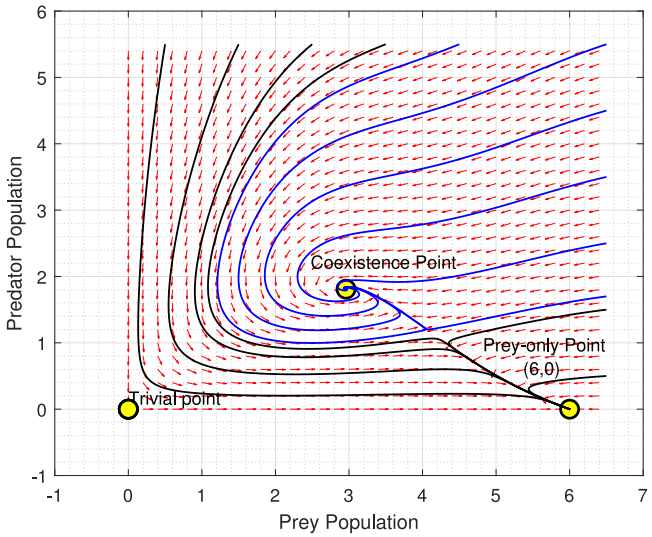

Fig. 6. Phase portrait of system (2) when condition (16) violated.

such that the number of predators exceeds the prey. This represents a state of lack of prey. The last point was chosen to represent the case in which the number of prey is equal to the number of predators. This diverse set of initial conditions was chosen to closely examine potentially unique behaviors and stability of the system under different realistic population density scenarios.

From Fig. 4, it is clear that irrespective of the initial conditions, all trajectories exhibited convergence towards the coexistence point. The result presented in this study offers robust empirical support for the global stability of the coexistence point which was obtained in the global stability Theorem 5. A globally stable equilibrium point signifies that any solution originating in close proximity to the equilibrium will ultimately converge towards and persist in the vicinity of the equilibrium indefinitely. In the present scenario, the confirmation of global stability is derived from the convergence of all trajectories towards the coexistence point. The findings of this study have substantial implications for the enduring dynamics of the system, indicating that the populations of predators and prey will maintain a stable coexistence over an extended period.

The time series plot that is shown in Fig. 5 provides a visual representation of the system's dynamic behavior over a period of time, illustrating the fluctuations and interrelationships between the populations of predators and prey. Over the period of time, the populations exhibit oscillatory behavior, indicating a state of equilibrium in the interaction between the two species. The observed oscillations serve as evidence for a persistent coexistence, wherein the dynamics of the predator and prey populations mutually influence one another.

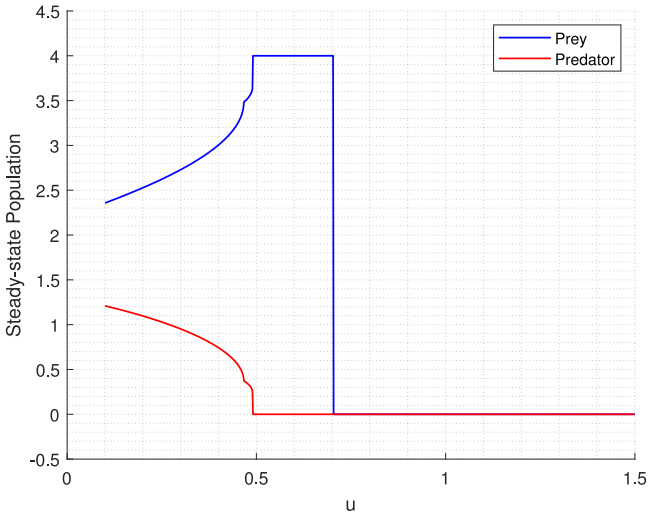

Fig. 7. Bifurcation analysis of system (2) at u. (For interpretation of the references to color in this figure legend, the reader is referred to the web version of this article.)

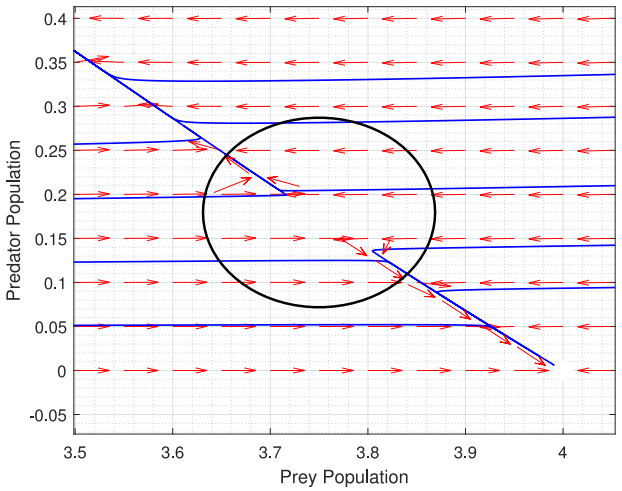

Fig. 8. Saddle–node bifurcation of system (2) when $u = 0.48$.

The observed consistent pattern in the time series analysis that is shown in Fig. 5 provides empirical evidence supporting the stability and robustness of the coexistence phenomenon within the system. The empirical evidence strongly supports the global stability of the prey–predator dynamics due to the convergence of trajectories. The aforementioned observations enhance comprehension of the extended-term dynamics and ecological dynamics of the system, emphasizing the importance of coexistence in upholding the overall stability and equilibrium within the ecosystem.

The observation of the non-compliance of the condition (16) in the simulation outcomes offers additional understanding of the system's dynamics and reinforces the credibility of the condition in ensuring global stability. When the condition is breached, indicating that the prey population is not adequately large in relation to the carrying capacity, the dynamics of the predator and prey populations demonstrate behavior that deviates from the coexistence point as shown in Fig. 6.

In instances of this nature, the population trajectories exhibit a tendency to deviate from the coexistence point, thereby suggesting an unstable or unsustainable dynamic as shown in black trajectories in Fig. 6. The aforementioned observation is consistent with the condition outlined in the global stability Theorem 5, which indicates that the stable coexistence of the prey–predator system requires a prey population of significant size.

The black trajectories that deviate from the coexistence point in contravention of the specified condition serve to illustrate the system's susceptibility to variations in both the initial conditions and parameter values. This underscores the significance of maintaining an appropriate equilibrium between predator and prey populations in order to achieve stable coexistence.

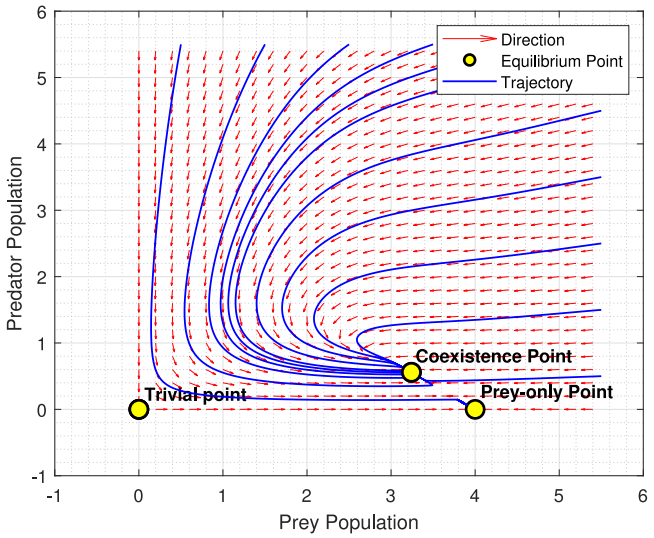

Fig. 9. The phase portrait of system (2) with $u = 0.5$.

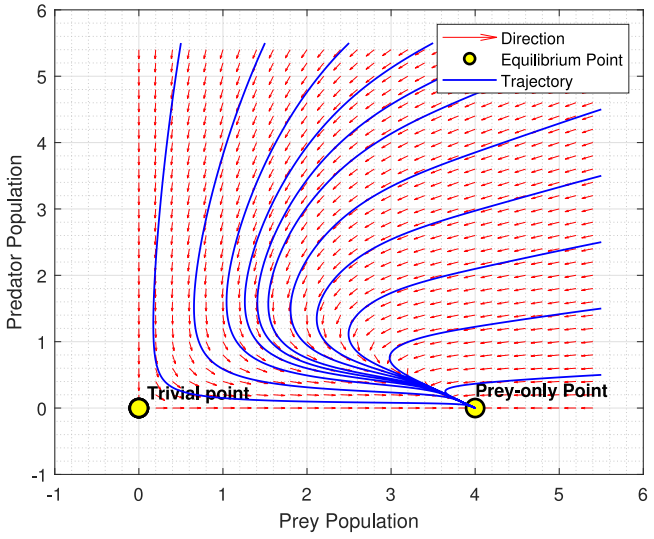

Fig. 10. The phase portrait of system (2) with $u = 0.9$.

The bifurcation analysis that conducted on the parameter u reveals intriguing dynamics within the system. As illustrated in Fig. 7 when the parameter u exceeds 0.47, a bifurcation occurs in the system, leading to a notable alteration in the steady-state populations of both the prey and predator.

The bifurcation diagram in Fig. 7 effectively depicts the behavior of the parameter u, where it is presenting the population levels of the prey (represented by blue) and the predator (represented by red) as a function of the parameter u.

Initially, when u assumes less than 0.47, the system demonstrates a state of stable coexistence, wherein both populations are observed to coexist in a harmonious equilibrium.

Nevertheless, when the value of u exceeds the critical threshold of 0.47, the system experiences a bifurcation. The bifurcation point signifies a significant shift in the system's behavior. At first when $u = 0.48$ the trajectories exhibit a departure from the coexistence point, leading to a notable alteration in the steady-state populations of both the prey and predator, where saddle–node bifurcation appears, as shown in Fig. 8.

The system undergoes a transition to another state, which is distinguished by the presence of a prey-only equilibrium point. In this state, the predator population declines to zero, while the prey population continues to exist as illustrated in Figs. 9 and 10 where the value of u is changed to 0.5 and 0.9 respectively.

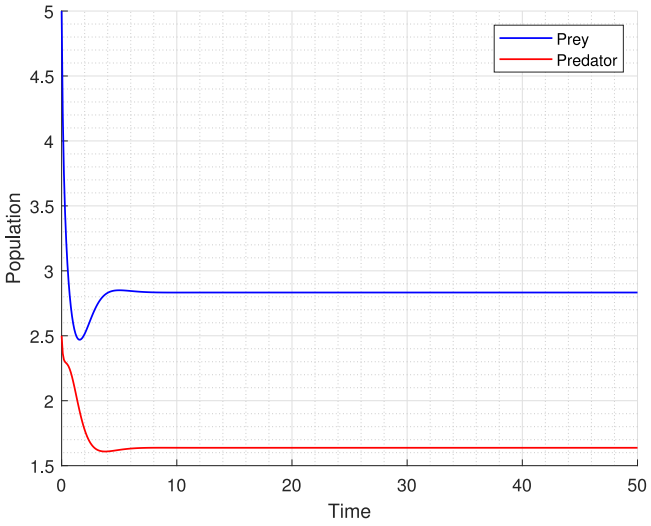

Fig. 11. Time series of system (2) with $j = 0, x_0 = 5$, and $y_0 = 2.5$.

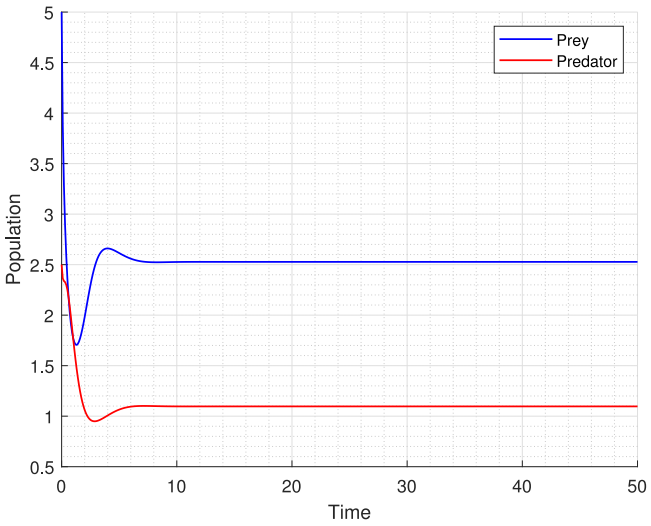

Fig. 12. Time series of system (2) with $j = 0.7, x_0 = 5$, and $y_0 = 2.5$.

The observed trajectory deviation from the point of coexistence and the appearance of the prey-only point emphasizes the importance of the parameter u in determining the dynamics and stability of the prey–predator system. It means that the value of u plays a crucial role in the persistence or extinction of the predator population and affects the overall dynamics of the system.

In the context of the prey–predator system, the parameter j holds a crucial significance as it quantifies the population size of predators that possess the capability to engage in predation effectively.

When the value of parameter j is assigned as zero ($j = 0$), time series simulations exhibit a noteworthy state of coexistence between the prey and predator, as illustrated in Fig. 11. In this particular scenario, the populations of both species coexist in a state of equilibrium. The predators, however, exhibit reduced proficiency in predation as a result of the absence of highly skilled individuals. As a result, the population of prey remains relatively constant, resulting in a correspondingly moderate population of predators.

However, a notable change is observed when a non-zero value is assigned to j, specifically $j = 0.7$, as illustrated in Fig. 12. In this particular instance, the analysis illustrates a decline in the prey population, which subsequently impacts the predator population, causing a reduction in their population as well. Additionally, the continuing to increase in the coefficient associated with increased predation skill leads to a substantial, consistent drop in both prey and predator populations over the long term, as shown in Fig. 13.

On the other hand, the analysis of parameter m, which represents the number of preys that had an opportunity to escape away or hide, unveils intricate ecological dynamics within the system. By examining the parameter m and its ecological implications, significant insights are gained into the interplay between species, revealing the nuanced mechanisms that contribute to the overall

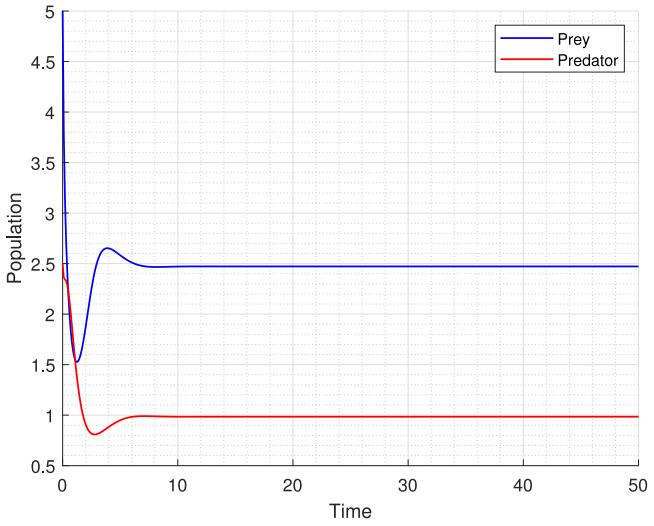

Fig. 13. Time series of system (2) with $j = 0.9, x_0 = 5$, and $y_0 = 2.5$.

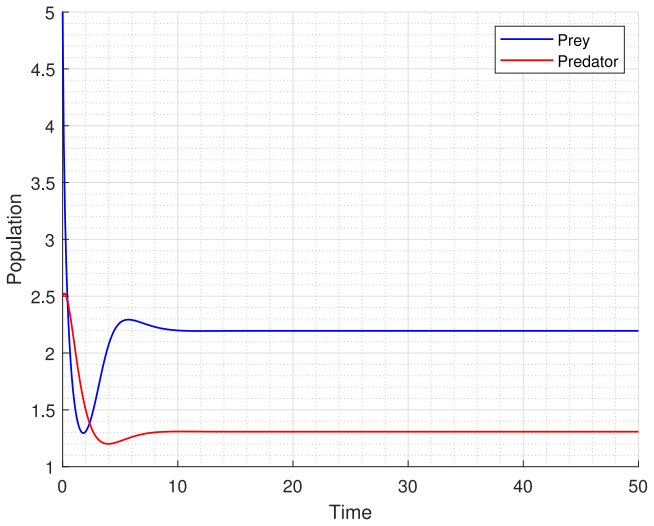

Fig. 14. Time series of system (2) with $m = 0, x_0 = 5$, and $y_0 = 2.5$.

stability and functioning of the ecosystem. It was noticed that the increasing in the value of m leads to an increase in the number of preys, but at the same time, it leads to a decrease in the number of predators as shown in Figs. 14, 15 and 16, where m is equal to $0, 0.5$, and 0.9 respectively.

The implications of the prey that had an opportunity to escape away or hide on population dynamics highlight on the equilibrium inherent in prey–predator relationships. The increasing m allows a greater number of preys to successfully evade predation, resulting in an augmented prey population size. As a result, the predator population undergoes a decline due to a decrease in successful predation events. Based on this premise, in some cases, when the growth rate of the prey decreases with the increasing m, it leads to a decay in the number of the predators. This occurs because the predator relies entirely on the presence of the prey for its reproduction, and also because of the isolated environment in which the prey and the predator live, as shown in Fig. 17.

The previously mentioned effectiveness possesses significant implications for the stability and persistence of the ecological system, as it exerts an influence on the abundance and spatial arrangement of species within the ecological community.

8. Conclusion

Through a series of theoretical and numerical analyses, the intricate dynamics of the ecological system have been studied. Theoretically, a complete analysis of the proposed ecosystem identified three positive equilibrium points, with the trivial point

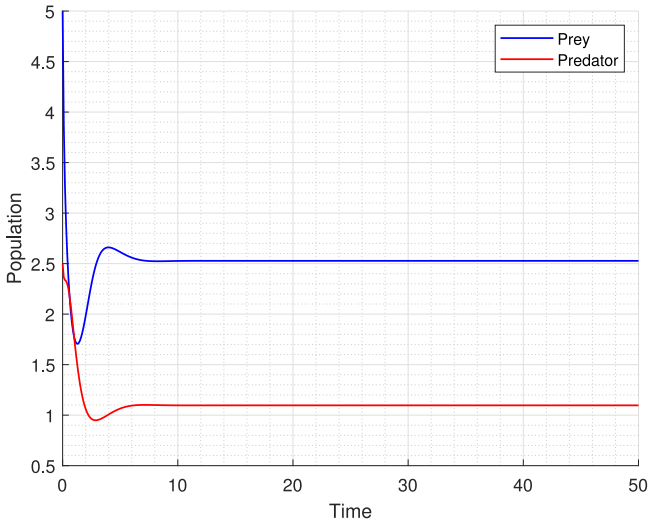

Fig. 15. Time series of system (2) with $m = 0.5, x_0 = 5,$ and $y_0 = 2.5$.

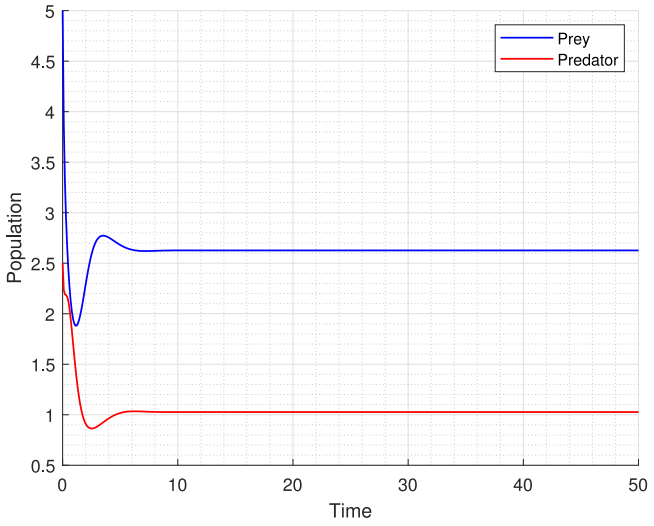

Fig. 16. Time series of system (2) with $m = 0.9, x_0 = 5,$ and $y_0 = 2.5$.

determined as unstable. The prey-only equilibrium point is locally stable under $\frac{eak}{1+ahk} < u + m(1 + \cos(k))$. The coexistence point exhibited stability under $\bar{x} > \frac{k}{2}$ and $\bar{x} < 2\bar{y}$. The global stability condition also serves as a local stability condition for the coexistence point, indicating the resilience of this condition. Applying Kolmogorov conditions, it was concluded that the system maintains coexistence when $k > \frac{u+\delta}{ea-ah\delta-ahu}$. Investigation of parameter u revealed a trans-critical bifurcation at the prey-only equilibrium and a saddle–node bifurcation at the coexistence equilibrium. Numerical simulations validated the occurrence of instability when stability conditions are violated. Numerical bifurcation analysis on parameter u identified a bifurcation threshold at $u = 0.47$, indicating a qualitative change in the system's dynamics. Simulations also highlighted the impact of parameters m and j. An increase in m, representing prey that can escape or hide, led to higher prey populations and reduced predator numbers. Increasing j, representing predators acquiring predation skills, caused a decrease in both prey and predator populations. These findings emphasize the sensitivity of the system to changes in m and j, underscoring the importance of managing these parameters for balanced coexistence.

Future research should integrate real-world data for model accuracy, investigate the influence of other environmental factors (e.g., prey age, time delay, diseases), extend the model to include multi-species interactions and spatial dynamics, and study the impacts of human interventions (e.g., protected areas, pollution, poaching). This work is limited by theoretical assumptions and simplified models, which may overlook real ecosystem complexities and face uncertainties in parameter estimation due to the dynamic nature of ecological systems.

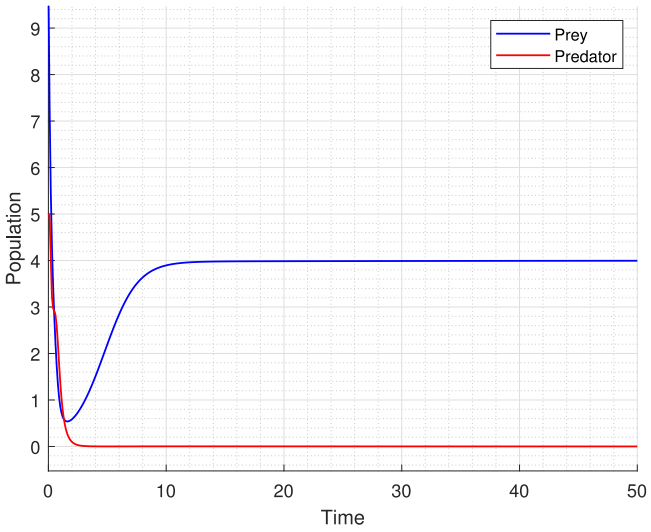

Fig. 17. Time series of system (2) with $m = 1.2, r = 0.7, x_0 = 5,$ and $y_0 = 2.5$.

Funding

The author received no direct funding for this work.

Declaration of competing interest

The authors declare that they have no known competing financial interests or personal relationships that could have appeared to influence the work reported in this paper.

Data availability

No data was used for the research described in the article.

References

[1] Hofbauer J, Sigmund K. Evolutionary games and population dynamics. Cambridge University Press; 1998.
[2] Lotka AJ. Elements of physical biology. Williams & Wilkins; 1925.
[3] Volterra V. Variazioni e fluttuazioni del numero d'individui in specie animali conviventi. Societá anonima tipografica Leonardo Vinci 1927;2:1–85.
[4] Alebraheem J. Dynamics of a predator–prey model with the effect of oscillation of immigration of the prey. Diversity 2021;13(1):23.
[5] Solomon ME. The natural control of animal populations. J Anim Ecol 1949;1–35.
[6] Holling CS. Some characteristics of simple types of predation and parasitism1. Can Entomol 1959;91(7):385–98.
[7] Ricklefs RE, Relyea R, Richter. Ecology: The economy of nature. New York: WH Freeman; 2014.
[8] Holling CS. The components of predation as revealed by a study of small-mammal predation of the European Pine Sawfly1. Can Entomol 1959;91(5):293–320.
[9] Ivlev VS. Experimental ecology of the feeding of fishes. Yale University Press; 1961.
[10] DeAngelis DL, Goldstein RA, O'Neill RV. A model for tropic interaction. Ecology 1975;56(4):881892.
[11] Varley GC, Gradwell GR, Hassell MP. Insect population ecology: An analytical approach. Univ of California Press; 1974.
[12] Li SB, Wu JH. Effect of cross-diffusion in the diffusion prey-predator model with a protection zone. Discrete Contin Dyn Syst 2017;37(3):1539–58.
[13] Pal S, Pal N, Samanta S, Chattopadhyay J. Effect of hunting cooperation and fear in a predator–prey model. Ecol Complex 2019;39:100770.
[14] Sekerci Y. Climate change effects on fractional order prey-predator model. Chaos Solitons Fractals 2020;134:109690.
[15] Emery SE, Mills NJ. Effects of predation pressure and prey density on short-term indirect interactions between two prey species that share a common predator. Ecol Entomol 2020;45(4):821–30.
[16] Al Basir F, Tiwari PK, Samanta S. Effects of incubation and gestation periods in a prey-predator model with infection in prey. Math Comput Simulation 2021;190:449–73.
[17] Jayaprakasha PC, Baishya C. Numerical analysis of predator–prey model in presence of toxicant by a novel approach. J Math Comput Sci 2021;11(4):3963–83.
[18] Lemnaouar MR, Benazza H, Khalfaoui M, Louartassi Y. Dynamical behaviours of prey-predator fishery model with two reserved area for prey in the presence of toxicity and response function Holling Type IV. J Math Comput Sci 2021;11(3):2893–913.
[19] Dawud S, Jawad S. Stability analysis of a competitive ecological system in a polluted environment. Commun Math Biol Neurosci 2022;2022. Article ID 70.
[20] Arif GE, Alebraheem J, Yahia WB. Dynamics of predator–prey model under fluctuation rescue effect. Baghdad Sci J 2023.
[21] Bhatt BS, Khan QJA, Jaju RP. Switching effect of predation on large size prey species exhibiting group defense. Differ Equ Control Process 1999;3.
[22] Söderbacka GJ. Model map and multistability for a two predator-one prey system. Differ Equ Control Process 2023.

[23] Jawad S, Naji RK. The influence of stage structure and prey refuge on the stability of the predator–prey model. Int J Eng Manuf 2022;12(3):51.
[24] Alalhareth FK, Atta U, Ali AH, Ahmad A, Alharbi MH. Analysis of leptospirosis transmission dynamics with environmental effects and bifurcation using fractional-order derivative. Alex Eng J 2023;80:372–82.
[25] Kulachi MO, Ahmad A, Hincal E, Ali AH, Farman M, Taimoor M. Control of conjunctivitis virus with and without treatment measures: A bifurcation analysis. J King Saud Univ-Sci 2024;103273.
[26] Ali A, Jawad S, Ali AH, Winter M. Stability analysis for the Phytoplankton-Zooplankton model with depletion of dissolved oxygen and strong Allee effects. Results Eng 2024;102190.
[27] LIMA, Steven L. Predators and the breeding bird: behavioral and reproductive flexibility under the risk of predation. Biol Rev 84(3):485–513.
[28] Caro T. Antipredator defenses in birds and mammals. University of Chicago Press; 2005.
[29] Biro PA, Beckmann C, Stamps JA. Small within-day increases in temperature affects boldness and alters personality in coral reef fish. Proc R Soc B Biol Sci 2010;277(1678):71–7.
[30] Thaker M, Vanak AT, Owen CR, Ogden MB, Niemann SM, Slotow R. Minimizing predation risk in a landscape of multiple predators: effects on the spatial distribution of African ungulates. Ecology 2011;92(2):398–407.
[31] Perko L. Differential equations and dynamical systems. Springer Science & Business Media; 2013.